FOCUS ON HEALTH

Radiography and Clinical Technology

Self-study CPD activity

Activity Reference Number:
A4(26) 2030

Topic

Metal Artifacts

Article(s)

Devising a novel evaluation method for computed tomography images containing metal artifacts from titanium seed implants: Application to virtual monochromatic imaging energy optimization

Speciality

CT / Radiation Oncology

Profession(s)

Radiographer
Radiologist

You can complete any one, or all the parts of this activity

Part 1 is approved for **TWO (2)** ***Clinical*** Continuing Education Units (CEU's)

Part 2 is approved for **TWO (2)** ***Clinical*** Continuing Education Units (CEU's)

Radiography 31 (2025) 102944

Contents lists available at ScienceDirect

Radiography

journal homepage: www.elsevier.com/locate/radi

Devising a novel evaluation method for computed tomography images containing metal artifacts from titanium seed implants: Application to virtual monochromatic imaging energy optimization

S. Kitaguchi [a, b, *], K. Imai [a], N. Hashimoto [b], K. Fujii [a], C. Yamauchi-Kawaura [a], T. Mizutani [b]

[a] Department of Integrated Health Sciences, Nagoya University Graduate School of Medicine, 1-1-20, Daiko-Minami, Higashi-ku, Nagoya, Aichi 461-8673, Japan

[b] Department of Central Radiology, Kindai University Hospital, 377-2 Ohno-Higashi, Osakasayama, Osaka 589-8511, Japan

ARTICLE INFO

Article history:
Received 15 November 2024
Received in revised form
18 March 2025
Accepted 21 March 2025
Available online 7 April 2025

Keywords:
Metal artifacts
Dual-energy computed tomography
Virtual monochromatic imaging
Contrast-to-artifact ratio
Brachytherapy

ABSTRACT

Introduction: Metal artifact reduction (MAR) technology cannot fully eliminate metal artifacts from metallic devices in computed tomography (CT) images. Hence, it is important to investigate the optimal acquisition parameters and post-processing techniques. This study aimed to devise a novel evaluation method for images containing metal artifacts from titanium seed implants and identify the optimal energy level for virtual monochromatic imaging (VMI) to reduce metal artifacts and enhance signal detectability.
Methods: Post-brachytherapy CT scans are a clinical example of the effects of metal artifacts. Therefore, we focused on the pelvic region, including the prostate, and created a phantom with simulated radioactive seeds that were inserted into the prostate region. We investigated the relationship between metal artifacts and monochromatic energy levels (35–200 keV at 5 keV intervals) using a dual-energy CT system with deep learning (DL) and MAR algorithms. Metal artifacts were investigated using the Gumbel evaluation method, which quantitatively evaluates artifacts, and contrast detectability was assessed using the contrast-to-noise ratio (CNR) and a newly devised contrast-to-artifact ratio (CAR).
Results: The location parameter, representing the physical index of metal artifacts, was the lowest at 65 keV. CNR and CAR achieved the highest signal detectability at 70 and 65 keV, respectively. VMI at 65 keV provided an optimal balance. When two images with similar CNR values were assessed using CAR, the resulting difference aligned consistently with the visual evaluation findings.
Conclusions: VMI at 65 keV with DL and MAR reconstructions is the optimal acquisition parameter for reducing metal artifacts and improving signal detectability. Additionally, CAR can be used to evaluate images affected by metal artifacts.
Implications for practice: CAR is useful for evaluating the effect of metal artifacts on signal detection.

Introduction

The use of metal devices within the body, such as artificial joints and implanted heart devices, has recently increased,[1,2] as has the number of X-ray computed tomography (CT) examinations for patients with metal devices. Metal devices exhibit extremely high linear attenuation coefficients, resulting in the rapid attenuation of X-rays. This attenuation causes X-ray beam hardening and photon starvation, producing metal artifacts in the CT images. These artifacts, characterized by image defects around the metal and the appearance of black and white streaks on the image, pose significant challenges in diagnostic imaging. Since the introduction of metal artifact reduction (MAR) technology in 2010,[3–6] notable improvements have been observed in addressing the inaccuracies

Abbreviations: AEC, automatic exposure control; CAR, contrast-to-artifact ratio; CNR, contrast-to-noise ratio; CT, computed tomography; DICOM, digital imaging and communication in medicine; DL, deep learning; DLR, deep learning reconstruction; HU, Hounsfield units; keV, kiloelectron volt; MAR, metal artifact reduction; ROI, region of interest; VMI, virtual monochromatic imaging.

* Corresponding author. Department of Central Radiology, Kindai University Hospital, 377-2 Ohno-Higashi, Osakasayama, Osaka 589-8511, Japan.

E-mail addresses: s-kitaguchi@med.kindai.ac.jp (S. Kitaguchi), imai@met.nagoya-u.ac.jp (K. Imai), n-hashimoto@med.kindai.ac.jp (N. Hashimoto), fujii@met.nagoya-u.ac.jp (K. Fujii), kawaura@met.nagoya-u.ac.jp (C. Yamauchi-Kawaura), takam35826@yahoo.co.jp (T. Mizutani).

https://doi.org/10.1016/j.radi.2025.102944

in imaging and information caused by artifacts from metal devices. Furthermore, most reports[7–11] on MAR have used dual-energy modes, such as the dual-source CT system (Siemens Healthcare, Forchheim, Germany) and virtual monochromatic imaging (VMI) obtained from a fast kilovoltage switching CT system (GE Healthcare, Waukesha, Wisconsin, USA), which are effective in reducing metal artifacts. Recent developments include a CT system that integrates a fast voltage-switching mode with deep learning (DL) technology.[12] The VMI obtained from this system may offer further potential for MAR applications.

Currently, the quality of radiological images, such as CT images, has been evaluated based on both subjective and quantitative assessments. One representative index for the quantitative evaluation of image quality is the contrast-to-noise ratio (CNR). CNR is a physical index for evaluating contrast detectability and is defined as a quantitative measure of the effect of noise on signal detection. Contrastingly, there is no index for evaluating the effect of metal artifacts on signal detection, and only subjective evaluation is performed. Therefore, it is useful to derive an index for evaluating the effect of metal artifacts on signal detection, and the impact of artifacts on signal detection can be evaluated by replacing the noise component with an indicator related to the artifacts.

In this study, we devised a new evaluation index, the contrast-to-metal artifact ratio (CAR), and investigated the optimal monochromatic energy level of VMI in CT images of metal-containing objects.

Methods

Phantom design

CT scans performed after brachytherapy are a clinical example of the effects of metal artifacts on image quality. Post-brachytherapy CT scans were performed the next day and one month later after brachytherapy at our institution to identify the location of the radioactive seed implants, confirm that the radioactive seed implants did not deviate from the prostate, and evaluate the dose distribution for radioactive seed implants using CT images. Accurate delineation of the prostate gland from surrounding organs, such as the rectum, bladder, and urethra, is essential.[13] However, metal artifacts from radioactive seed implants often cause image defects, complicating each organ's precise tracing. Therefore, this study focused on the pelvic region, including the prostate, and a phantom was created to simulate this region. Fig. 1 shows a schematic of the target analysis used in this study. The phantom was designed to mimic both the soft tissue and prostate region. Agar was used as the base material to simulate soft tissue and prostate regions.

As shown in Fig. 1, the agar that simulated soft tissue was placed in an elliptical container with dimensions of 290 × 225 mm and a thickness of 120 mm. The prostatic region was centrally located in the container. In many studies, iodine contrast medium has been used to adjust CT values to simulate soft tissues and organs of the body. However, contrast media cannot simulate energy-independent soft tissues because the absorbed X-ray dose varies with energy. Therefore, we reproduced energy-independent soft tissue by mixing sucrose-dissolved water within the agar and varying the sucrose water concentration to achieve a soft tissue CT value of 10 Hounsfield units (HU), and the CT value of the prostate region was set to 50 HU. Fig. 2 shows the monochromatic energy dependence of the image contrast for VMI, which was defined as the difference in CT numbers between the simulated tissue and prostate. The image contrast was almost constant regardless of the monochromatic energy and was estimated to be approximately 40 HU (50 HU -10 HU). Furthermore, the characteristics of the image

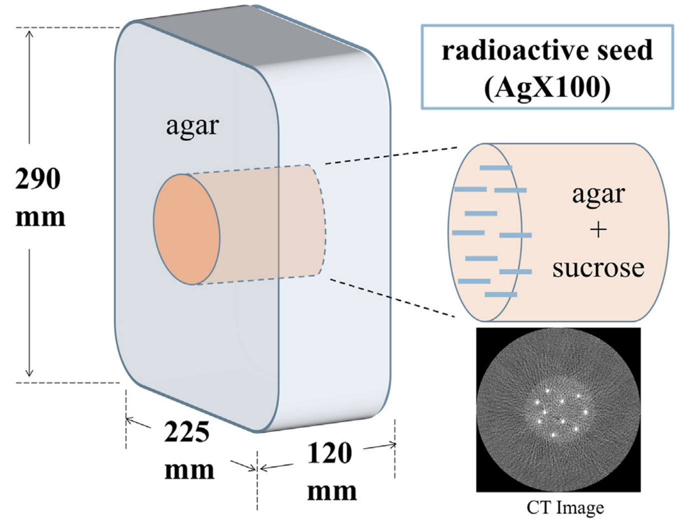

Figure 1. Representation of the phantom used in this study. The phantom simulated soft tissue and prostate tissue. Titanium simulated radioactive seeds for brachytherapy were inserted into the prostate region.

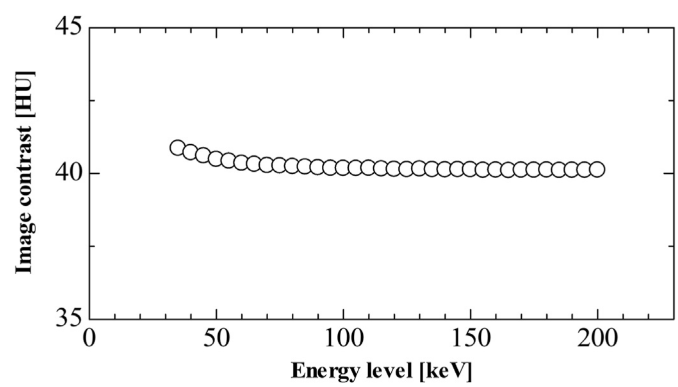

Figure 2. Monochromatic energy dependence of image contrast. The graph indicates the image contrast between ROI1 and ROI2 for each energy level. The image contrast was approximately 40 HU at each energy level.
ROI, region of interest; HU, Hounsfield units.

contrast did not vary before and after the phantom study. The CT numbers of human soft tissue are known to remain almost constant, regardless of monochromatic energy. Therefore, our abdominal phantom exhibited a monochromatic energy dependence similar to that of soft tissues.

In this study, ten titanium radioactive seed implants (Sera AgX100; Nihon Medi-Physics, Tokyo, Japan) without I-125, measuring 4.5 × 0.8 mm, used in prostate cancer brachytherapy, were prepared as generation sources of metal artifacts and inserted into the prostate region of the abdominal phantom. The CT image in Fig. 1 represents the metal artifacts originating from radioactive seed implants.

VMI acquisition

Phantom images were acquired using the dual-energy mode of a 320-row area-detector CT system installed at our institution (Aquilion ONE Nature Edition Ver. 10.12; Canon Medical Systems, Tochigi, Japan). The acquisition parameters are presented in Table 1. After acquiring the raw data, the reference material image was reconstructed using the DL reconstruction (DLR) and MAR

Table 1
Summary of computed tomography (CT) acquisition and image reconstruction parameters.

Acquisition and reconstruction parameters	
CT System	320-row area-detector CT (Aquilion ONE: Canon Medical Systems)
Scan mode	Dual Energy Helical Scan
Detector cofiguration	0.5 mm × 80 rows
Tube voltage (kVp)	80 and 135 kVp (Rapid kV switching method)
Target standard deviation value for automatic exposure control[a]	8 (for 0.5 mm thickness images)
Helical pitch	65.0
Rotation speed (s/rotation)	0.5
Acquisition field-of-view (mm)	350
CTDI: (mGy · cm)	14.9
DLP: (mGy · cm)	123.40
Reconstruction method	Deep Learning Spectral Reconstruction
Reconstruction kernel	AiCE[b] Body Mild
Reconstruct slice thickness (mm)	2.0
Reconstruct field-of-view (mm)	120
Image matrix	512 × 512
Energy level of VMI reconstruction (keV)	35-200 (5 increments)
Clinical Applications	Metal artifact reduction (SEMAR[c])

[a] Automatic exposure control estimates the image quality level in terms of the standard deviation of CT numbers (SD, noise level) and determines the tube current.
[b] AiCE: Advanced Intelligent Clear-IQ Engine.
[c] SEMAR: Single Energy Metal Artifact Reduction.

algorithms. Subsequently, VMI ranging from 35 to 200 keV at 5 keV intervals were generated from the reference material image using a medical-image-processing workstation (Vitrea Ver. 8.10; Canon Medical Systems, Tochigi, Japan). The VMI was converted to a Digital Imaging and Communication in Medicine file for artifact analysis.

Analysis method

Fig. 3 shows an example of an image used to evaluate metal artifacts, which appear as black and white streaks originating from the metal substances. In the present study, the region of interest (ROI) measurement was a square of 40 × 40 pixels set on the CT image (Fig. 3). Forty CT value profiles obtained from ROI_1 measurement were used to analyze the metal artifacts. Metal artifacts were evaluated using the Gumbel evaluation method devised by Imai et al..[14–17] The Gumbel evaluation method, an analysis technique based on the Gumbel distribution,[18] focuses on the extreme values. The metal artifacts were evaluated by block sampling the largest CT value variations within the ROI measurement and using location parameters as physical indicators. A brief description of this method, adapted from Imai et al.,[14] is as follows: The largest difference between adjacent CT values, which is the value calculated from the CT value profile in each profile, was used as the random variable (x). The cumulative probability function for x, denoted as $F(x)$, is expressed as

$$F(x) = exp\left[- exp\left(-\frac{x-\beta}{\gamma} \right) \right] \quad (1)$$

where β and γ are the location and scale parameters, respectively, with the location parameter corresponding to the mode and the scale parameter corresponding to the variance of the distribution. The unknown cumulative probability function can also be estimated using the mean rank method[18,19] with "order statistics." Thus, the largest difference between adjacent CT values was arranged in ascending order: $x(1) \le x(2) \le \ldots \le x(40)$, and $F(x_{(i)})$ was computed as

$$F\left(x_{(i)}\right) = \frac{i}{n+1} \quad (2)$$

where n is the sample size (40 in this study). The location parameterβ and the scale.

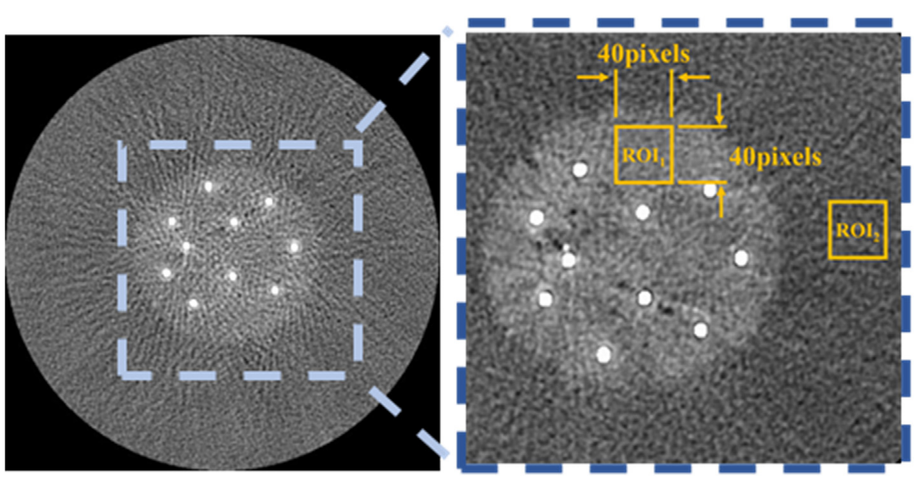

Figure 3. The location of the ROIs placed on the analyzed image. Target CT images, which obtained using the dual-energy CT scanner with deep learning technology, analyzed metal artifacts and signal detectability. The measurements ROI_1 and ROI_2 were set in regions on the analyzed image that simulated soft tissue and the prostate, respectively.
ROI, region of interest; CT, computed tomography.

Parameter γ was estimated by line-fitting on the Gumbel plot and used as a physical index for evaluating metal artifacts on CT images.

Evaluation of signal detectability by CNR

Signal detectability, which is the ability to distinguish an image signal on a CT image, was quantitatively assessed using the CNR, which measures the difference between image signals and noise. CNR, a physical index of contrast resolution, is defined by Equation (3) and is often used in clinical settings.

$$CNR = \frac{CT \quad ROI_1 - CT \quad ROI_2}{Noise \quad SD} \tag{3}$$

where CT ROI_1 is the mean CT number of ROI_1, CT ROI_2 is the mean CT number of ROI_2, and Noise SD is the standard deviation of the CT values in ROI_2. The CNR for each monochromatic energy level was calculated using the following formula.

Evaluation of signal detectability by CAR

In this study, we devised a new physical index, the CAR, to evaluate the effect of metal artifacts on signal detectability. The CAR is defined similarly to the CNR but uses the location parameter of the Gumbel evaluation method as follows:

$$CAR = \frac{CT \quad ROI_1 - CT \quad ROI_2}{Artifact \quad value} \tag{4}$$

where CT ROI_1 is the mean CT number of ROI_1, CT ROI_2 is the mean CT number of ROI_2, and the artifact value represents the location parameter of ROI_1. The CAR at each energy level was calculated using the following equation.

Results

Fig. 4(a) illustrates the largest difference between the adjacent CT values for each monochromatic energy. In the Gumbel plots, the largest difference between the adjacent CT values was on the fitted straight line. Regardless of monochromatic energy, Pearson's correlation coefficients were estimated to be $r = 0.977–0.992$. These results indicate that metal artifacts can be statistically modeled using the Gumbel distribution. Fig. 4(b) depicts the relationship between the location parameter and the monochromatic energy. A minimum was reached at 65 keV in the energy dependence of the location parameters. Fig. 5(a) and (b) show the CNR and CAR as quantitative indices of the contrast detectability for the virtual monochromatic energy level, respectively. The CNR and CAR values for the virtual monochromatic energy level are also listed in Table 2. The evaluations of CNR and CAR revealed that the highest signal detectability was achieved at 70 keV for CNR and 65 keV for CAR. These results showed that the signal detectability improved by reducing metal artifacts, making the VMI reconstructed at 65 keV suitable for detecting image signals obscured by metal artifacts.

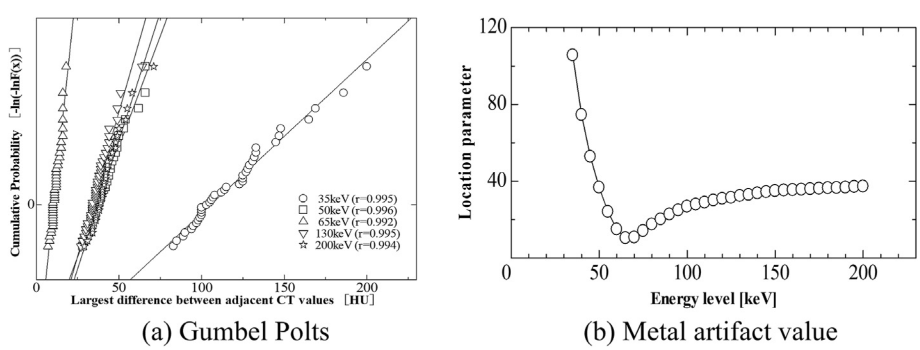

Figure 4. Result of Gumbel evaluation method. (a) Gumbel plots of the largest difference between adjacent CT values. The largest difference between adjacent CT values obtained at energy levels of 35, 50, 65, 130, and 200 keV in ROI_1 were plotted on the Gumbel probability paper. This plot is called the Gumbel plot. (b) The energy dependence of the location parameters of the Gumbel method. This graph depicts the relationship between location parameter and monochromatic energy level.
CT, computed tomography; keV, kiloelectron voltage; ROI, region of interest.

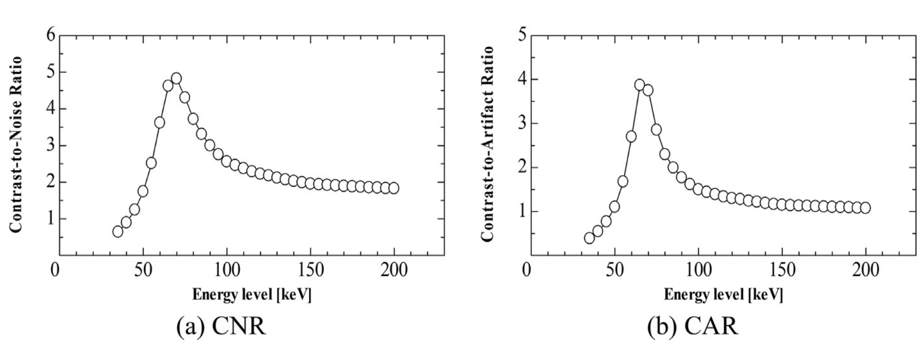

Figure 5. Relationship between contrast detectability and monochromatic energy level. Energy dependence of (a) CNR, which is generally used, and (b) CAR, which is newly devised.
CNR, contrast-to-noise ratio; CAR, contrast-to-artifact ratio.

Table 2
Results of quantitative evaluation for contrast detectability using contrast-to-noise ratio (CNR) and contrast-to-artifact ratio (CAR) at virtual monochromatic energy level. keV: kiloelectron volt.

keV	CNR	CAR	keV	CNR	CAR	keV	CNR	CAR
35	0.64	0.39	95	2.75	1.62	155	1.94	1.14
40	0.90	0.55	100	2.56	1.50	160	1.92	1.13
45	1.25	0.77	105	2.46	1.44	165	1.91	1.12
50	1.74	1.10	110	2.37	1.39	170	1.89	1.12
55	2.51	1.68	115	2.29	1.34	175	1.88	1.11
60	3.62	2.70	120	2.22	1.30	180	1.87	1.10
65	4.62	3.87	125	2.18	1.28	185	1.85	1.10
70	4.82	3.75	130	2.12	1.24	190	1.85	1.09
75	4.30	2.85	135	2.07	1.22	195	1.83	1.08
80	3.72	2.30	140	2.03	1.19	200	1.83	1.07
85	3.31	1.99	145	1.99	1.17			
90	3.00	1.77	150	1.95	1.15			

Discussion

The Gumbel evaluation method was used to evaluate the metal artifacts. The location parameter, a physical index that quantifies the extent of metal artifacts, was the smallest at 65 keV. Furthermore, when the actual images were verified (Fig. 6(a), (b), and 6(c)), visual confirmation revealed that the VMI at 35 and 135 keV was affected by artifacts from the simulated radioactive seed implants, whereas the VMI at 65 keV was the least affected. This suggests that the 65 keV energy effectively reduced the metal artifact effects. However, this finding differs from those of previous studies. Notably, Meinel et al.[8] confirmed that the optimal energy for titanium was 140 keV in subjective and objective assessments of metal artifacts in phantom VMI. Furthermore, an investigation of the effect of reducing metallic dental artifacts in clinical VMI reconstructed by the MAR algorithm reported that the margin and internal architecture of metallic dentures were more clearly delineated in higher-energy images than in lower-energy images.[7] Another study evaluated metal artifacts caused by pedicle screws in patients with scoliosis and found the optimal energy range to be between 110 and 140 keV.[10] We postulated that the difference in results from these studies was due to several factors, including the difference in the generation sources of metal artifacts and the use of DL technology in the CT system used in our study. This technology recovers missing projection data and estimates complete data when switching between two high and low tube voltages. Furthermore, the DLR algorithm was applied to reduce noise in the low-voltage data, resulting in highly accurate projection data with reduced noise. Because this technology differs from conventional dual-energy CT systems, we believe that a noise-reduced reference material image improves the accuracy of metal extraction and reduces metal artifacts, leading to differences in the results. However, conventional systems lack the advanced image reconstruction capabilities of the DLR.

The contrast detectability of the CNR and the proposed CAR were also evaluated. The results showed that the CNR and CAR were lower at 35 keV and higher at 65–70 keV, and decreased thereafter as the energy increased. Visually, signal detectability was reduced by VMI at 35 keV owing to artifacts, whereas VMI at 65 keV showed improved performance. Thus, the present study indicates that 65 keV is a useful energy band that offers the lowest metal artifacts and highest signal detectability. Furthermore, in dual-energy mode imaging, VMI in the 65–70 keV energy band is equivalent to 120 kVp image in single-energy mode.[9] This energy band is widely

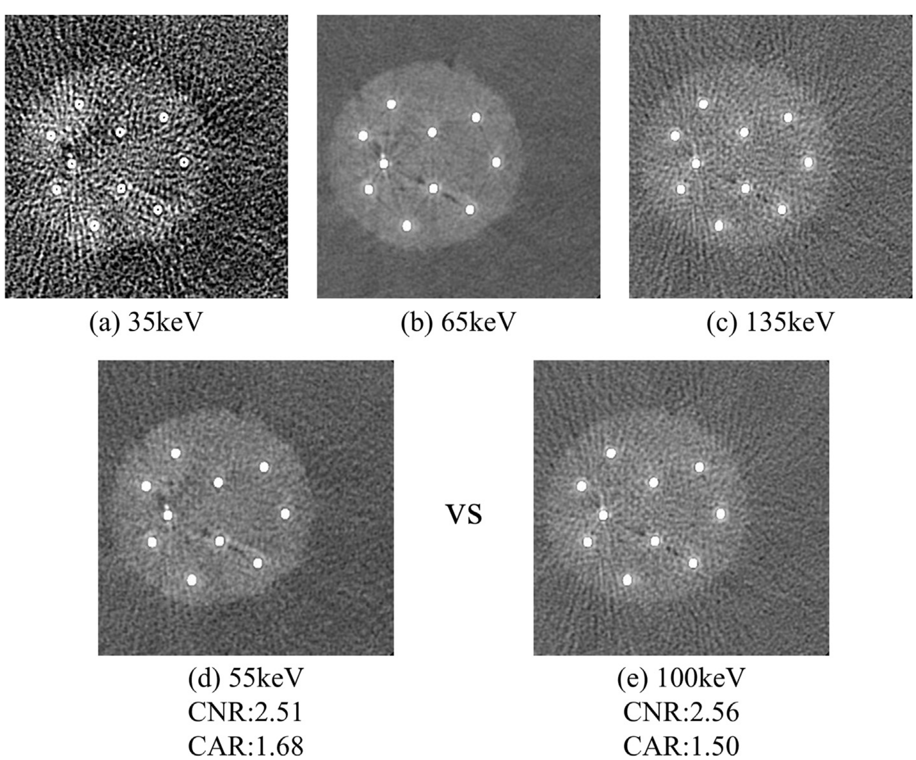

Figure 6. target VMI obtained at various monochromatic energy levels; (a) 35 keV, (b) 65 keV, and (c) 135 keV. The bottom row shows VMI at (d) 55 keV and (e) 100 keV, which CNR was almost equivalent. Value of CNR and CAR are shown. (Window level: 50 HU, Window width: 320 HU)
VMI, virtual monochromatic image; keV, kiloelectron voltage; CNR, contrast-to-noise ratio; CAR, contrast-to-artifact ratio.

used in routine clinical practice as a substitute for 120 kVp, which has been the standard since the advent of CT. Therefore, clinicians can make diagnoses without discomfort because they are familiar with single-energy mode images.

Based on these results, we recommend that the optimal scan parameters include the use of noise-reducing image reconstruction algorithms, such as DLR, to enhance metal extraction, apply MAR algorithms, and utilize VMI at 65 keV in dual-energy mode. These measures are essential for acquiring images with minimal metal artifact influence and high signal detectability. The highest peaks for CNR and CAR were observed at 70 and 65 keV, respectively. Similar trends across energy levels indicate that CAR can be used to evaluate the signal detection capability. Fig. 6(d) and (e) show examples of images used in this analysis, showing VMI at 55 and 100 keV, respectively. The CNR values were almost equivalent: 2.51 at 55 keV and 2.56 at 100 keV (Table 2). However, the CAR values differed, with 1.68 at 55 keV and 1.50 at 100 keV, respectively. Visually, the VMI at 100 keV displayed more metal artifacts and a rough texture, which negatively impacted the signal detectability. Thus, the proposed CAR may provide a more reliable assessment of signal detectability in images affected by metal artifacts.

This study had some limitations. First, the structure of the phantom used was significantly different from that of a human body. In clinical practice, metal artifacts may occur in the presence of various structures, such as bones, which may present different characteristics. Therefore, using a phantom that closely resembles human anatomy could yield more clinically relevant information. Second, in clinical CT examinations, not only titanium radioactive seed implants but also other metal devices, such as joint implants and metallic dental prostheses, are sources of metal artifacts. These metal devices may have different characteristics of metal artifacts from radioactive seed implants. Third, in this study, the effect of metal artifacts on contrast detectability in a simplistic phantom was quantitatively evaluated using the derived CAR. However, this index has not been applied to the evaluation of metal artifacts in clinical CT images. Additionally, no image reading examinations, such as the Likert scale and Receiver Operating Characteristic (ROC) analyses, were performed. Therefore, further investigations are necessary to provide clinical value to our study. Finally, the image acquisition method involved VMI reconstructed from raw data obtained using the dual-energy mode. When imaging is performed using a conventional tube voltage of 120 kVp, continuous X-rays cause an energy shift, commonly known as beam hardening, as they pass through the subject. To address this, CT manufacturers have implemented image quality compensation techniques, including the correction of CT numbers using algorithms and artifact reduction methods. Therefore, while the effect of metal artifacts on image quality may differ between VMI and conventional polychromatic CT images reconstructed using DLR and MAR algorithms, this study did not compare them. These limitations should be addressed in future studies.

Conclusions

In this study, we introduced the CAR as a new physical index for evaluating the impact of metal artifacts on contrast detectability and investigated the relationship between metal artifacts and monochromatic energy levels using a dual-energy CT scanner with DL. Consequently, the CAR was useful for evaluating the effect of metal artifacts on signal detection. Furthermore, we identified the use of noise-reducing image reconstruction algorithms, such as DLR, metal artifact reduction processes, and VMI at 65 keV, as optimal acquisition parameters for acquiring images with high signal detectability and minimal metal artifact influence.

Data availability

The datasets used and/or analyzed during the current study are available from the correspond-ing author on reasonable request.

Ethical approval and consent to participate

This article does not contain any studies with human participants or animals performed by any of the authors.

CRediT authorship contribution statement

Shigetoshi Kitaguchi: Writing – original draft, Conceptualization, Data curation, Formal analysis, Investigation, Validation, Visualization.
Kuniharu Imai: Writing – review & editing, Methodology, Supervision.
Naomi Hashimoto: Data curation, Investigation.
Keisuke Fujii: Writing – review & editing.
Chiyo Yamauchi-Kawaura: Writing – review & editing.
Takashi Mizutani: Conceptualization, Resources.

Conflict of interest statement

None

Acknowledgments

The authors express their deepest gratitude to the Department of Central Radiology and the Department of Radiology of Kinki University Hospital for their cooperation in conducting this study.

This research did not receive any specific grant from funding agencies in the public, commercial, or not-for-profit sectors.

References

1. Benito N, Esteban J, Horcajada JP, Ribera A, Soriano A, Sousa R. Epidemiology of prosthetic joint infection. In: Peel T, editor. *Prosthetic joint infections*. Cham: Springer International Publishing; 2018. p. 5–53.
2. Mond HG, Proclemer A. The 11th world survey of cardiac pacing and implantable cardioverter-defibrillators: calendar year 2009–A world society of arrhythmia's project. *Pacing Clin Electrophysiol* 2011;**34**(8):1013–27. https://doi.org/10.1111/j.1540-8159.2011.03150.x.
3. Li H, Noel C, Chen H, Harold Li H, Low D, Moore K, et al. Clinical evaluation of a commercial orthopedic metal artifact reduction tool for CT simulations in radiation therapy. *Med Phys* 2012;**39**(12):7507–17. https://doi.org/10.1118/1.4762814.
4. Morsbach F, Wurnig M, Kunz DM, Krauss A, Schmidt B, Kollias SS, et al. Metal artefact reduction from dental hardware in carotid CT angiography using iterative reconstructions. *Eur Radiol* 2013;**23**(10):2687–94. https://doi.org/10.1007/s00330-013-2885-z.
5. Gondim Teixeira PA, Meyer JB, Baumann C, Raymond A, Sirveaux F, Coudane H, et al. Total hip prosthesis CT with single-energy projection-based metallic artifact reduction: impact on the visualization of specific periprosthetic soft tissue structures. *Skelet Radiol* 2014;**43**(9):1237–46. https://doi.org/10.1007/s00256-014-1923-5.
6. Guilfoile C, Rampant P, House M. The impact of smart metal artefact reduction algorithm for use in radiotherapy treatment planning. *Australas Phys Eng Sci Med* 2017;**40**(2):385–94. https://doi.org/10.1007/s13246-017-0543-5.
7. Cha J, Kim HJ, Kim ST, Kim YK, Kim HY, Park GM. Dual-energy CT with virtual monochromatic images and metal artifact reduction software for reducing metallic dental artifacts. *Acta Radiol* 2017;**58**(11):1312–9. https://doi.org/10.1177/0284185117692174.
8. Meinel FG, Bischoff B, Zhang Q, Bamberg F, Reiser MF, Johnson TR. Metal artifact reduction by dual-energy computed tomography using energetic extrapolation: a systematically optimized protocol. *Investig Radiol* 2012;**47**(7):406–14. https://doi.org/10.1097/RLI.0b013e31824c86a3.
9. Neuhaus V, Große Hokamp N, Abdullayev N, Rau R, Mpotsaris A, Maintz D, et al. Metal artifact reduction by dual-layer computed tomography using virtual monoenergetic images. *Eur J Radiol* 2017;**93**:143–8. https://doi.org/10.1016/j.ejrad.2017.05.013.
10. Wang Y, Qian B, Li B, Qin G, Zhou Z, Qiu Y, et al. Metal artifacts reduction using monochromatic images from spectral CT: evaluation of pedicle screws in patients with scoliosis. *Eur J Radiol* 2013;**82**(8):e360–6. https://doi.org/10.1016/j.ejrad.2013.02.024.

11. Shinohara Y, Sakamoto M, Iwata N, Kishimoto J, Kuya K, Fujii S, et al. Usefulness of monochromatic imaging with metal artifact reduction software for computed tomography angiography after intracranial aneurysm coil embolization. *Acta Radiol* 2014;**55**(8):1015–23. https://doi.org/10.1177/0284185113510492.
12. Kojima T, Shirasaka T, Kondo M, Kato T, Nishie A, Ishigami K, et al. A novel fast kilovoltage switching dual-energy CT with deep learning: accuracy of CT number on virtual monochromatic imaging and iodine quantification. *Phys Med* 2021;**81**:253–61. https://doi.org/10.1016/j.ejmp.2020.12.018.
13. Nag S, Bice W, DeWyngaert K, Prestidge B, Stock R, Yu Y. The American Brachytherapy Society recommendations for permanent prostate brachytherapy postimplant dosimetric analysis. *Int J Radiat Oncol Biol Phys* 2000;**46**(1):221–30. https://doi.org/10.1016/S0360-3016(99)00351-X.
14. Imai K, Ikeda M, Wada S, Enchi Y, Niimi T. Analysis of streak artefacts on CT images using statistics of extremes. *Br J Radiol* 2007;**80**(959):911–8. https://doi.org/10.1259/bjr/93741044.
15. Imai K, Ikeda M, Enchi Y, Niimi T. Statistical characteristics of streak artifacts on CT images: relationship between streak artifacts and mA s values. *Med Phys* 2009;**36**(2):492–9. https://doi.org/10.1118/1.3056554.
16. Imai K, Ikeda M, Enchi Y, Niimi T. Quantitative assessment of image noise and streak artifact on CT image: comparison of z-axis automatic tube current modulation technique with fixed tube current technique. *Comput Med Imag Graph* 2009;**33**(5):353–8. https://doi.org/10.1016/j.compmedimag.2009.02.003.
17. Kitaguchi S, Imai K, Ueda S, Hashimoto N, Hattori S, Saika T, et al. Quantitative evaluation of metal artifacts on CT images on the basis of statistics of extremes. *Nippon Hoshasen Gijutsu Gakkai Zasshi* 2016;**72**(5):402–9. https://doi.org/10.6009/jjrt.2016_JSRT_72.5.402.
18. Gumbel EJ. *Statistics of extremes*. New York: Columbia University Press; 1958.
19. Johnson LG. *The statistical treatment of fatigue experiments*. New York: Elsevier; 1964.

QUESTIONNAIRE
A4(26) Part 1 of 2
Devising a novel evaluation method for computed tomography images containing metal artifacts from titanium seed implants: Application to virtual monochromatic imaging energy optimization

INSTRUCTIONS

- Read through the article and answer the multiple-choice questions provided below.
- All questions have only **ONE** correct answer

Question 1: Which one of the following was **NOT** one of the aims of the study?

A: Comparing CT and MRI for prostate imaging
B: To devise a novel method for evaluating metal artifacts from titanium seed implants
C: To identify the optimal energy level for VMI to reduce metal artifacts and enhance signal detectability
D: None of the above

Question 2: Which imaging technique was optimized in this study?

A: Single-energy CT
B: MRI
C: Virtual monochromatic imaging (VMI)
D: Ultrasound

Question 3: What type of metal implant was simulated in the phantom?

A: Titanium radioactive seed implants
B: Dental screws
C: Hip prosthesis
D: Cardiac stents

Question 4: What region of the body did the phantom simulate?

A: Thorax
B: Pelvic region including the prostate
C: Brain
D: Spine

Question 5: Which material was used to simulate soft tissue in the phantom?

A: Silicone
B: Gelatin
C: Saline solution
D: Agar mixed with sucrose water

Question 6: What does CNR stand for?

A: Contrast-to-resolution ratio
B: Contrast-to-radiation ratio
C: Contrast-to-noise ratio
D: Contrast normalization ratio

Question 7: What new metric was introduced in this study?

A: Contrast-to-artifact ratio (CAR)
B: Artifact-to-noise ratio
C: Metal-to-signal ratio
D: Artifact suppression index

Question 8: What statistical method was used to evaluate metal artifacts?

A: Gumbel evaluation method
B: ROC analysis
C: ANOVA
D: Chi-square test

Question 9: What does the location parameter in the Gumbel method represent?

A: Image contrast
B: Physical index of metal artifacts
C: Noise level
D: CT dose

Question 10: What was the optimal energy level for CAR?

A: 55 keV
B: 70 keV
C: 110 keV
D: 65 keV

THE END

QUESTIONNAIRE
A4(26) Part 2 of 2
Devising a novel evaluation method for computed tomography images containing metal artifacts from titanium seed implants: Application to virtual monochromatic imaging energy optimization

INSTRUCTIONS

- Read through the article and answer the multiple-choice questions provided below.
- All questions have only **ONE** correct answer

Question 1: What CT system was used in the study?

A: Siemens SOMATOM
B: GE Revolution CT
C: Canon Aquilion ONE
D: Philips iCT

Question 2: What was the tube voltage configuration?

A: 100 and 140 kVp
B: 80 and 120 kVp
C: 90 and 130 kVp
D: 80 and 135 kVp

Question 3: What was the slice thickness used for reconstruction?

A: 2.0 mm
B: 3.0 mm
C: 1.0 mm
D: 5.0 mm

Question 4: What reconstruction algorithm was applied?

A: Filtered back projection
B: Iterative reconstruction
C: Deep learning reconstruction (DLR)
D: MAR only

Question 5: What was the image matrix size?

A: 256 x 256
B: 512 x 512
C: 1024 x 1024
D: 640 x 640

Question 6: At which energy level was the location parameter lowest?

A: 70 keV
B: 55 keV
C: 65 keV
D: 100 keV

Question 7: What was the highest CNR value recorded?

A: 4.82
B: 3.62
C: 4.30
D: 5.00

Question 8: What was the approximate image contrast between ROI1 and ROI2?

A: 20 HU
B: 30 HU
C: 50 HU
D: 40 HU

Question 9: Which energy level showed the most visual reduction in metal artifacts?

A: 35 keV
B: 135 keV
C: 65 keV
D: 100 keV

Question 10: What was a key limitation of the study?

A: Lack of CT dose data
B: Phantom did not replicate human anatomy
C: No use of contrast media
D: Use of outdated CT system

THE END

FOCUS ON HEALTH
www.foh-cpd.co.za
Cell: 074 230 3874
Tel: 012 653 0133 / 2373 / 2394
Mon-Fri: 08:00-16:00

400 Theuns van Niekerk Street
Wierda Park
0157

PO Box 71
Wierda Park
0149

MEMBER INFO

(Complete sections marked with an asterisk *)

*FOH number		*HPCSA number	
ID number			
Personal detail changes			

I hereby declare that the completion of this document is my own effort without any assistance.

SIGNED: DATE:

This activity is accredited for **FOUR (4) CLINICAL** CEU'S. You have to achieve **70%** to pass this activity.

ANSWER SHEET

A4(26)

Devising a novel evaluation method for computed tomography images containing metal artifacts from titanium seed implants: Application to virtual monochromatic imaging energy optimization

***Time spent on activity hour min**

You can complete any one, or all the parts of this activity.

PART 1												**PART 2**											
	A	B	C	D	E		A	B	C	D	E		A	B	C	D	E		A	B	C	D	E
1						6						1						6					
2						7						2						7					
3						8						3						8					
4						9						4						9					
5						10						5						10					

How relevant was the content of this activity to your scope of practice?			
Not at all	Somewhat	Mostly	Extremely

RETURN ANSWER SHEET TO
Online members, complete your answer sheet online
CPD PORTAL: http://foh-cpd.co.za/cpd-online/cpd-user (Username: FOH number & Password: ID)
(Results are available immediately)

Email or hard copy members, complete your answer sheet online or return it to:
WHATSAPP: 074 230 3874 EMAIL: info@foh-cpd.co.za
(Results will be sent via email)

You will receive a confirmation of receipt either by Whatspp or email within 12-24hours, if not received please send again.

Have a suggestion or comment?

Send it to us on EMAIL or WHATSAPP